scientific reports

Check for updates

OPEN

Fe_3O_4@SiO_2@KIT-6@2-ATP@Cu^I as a catalyst for hydration of benzonitriles and reduction of nitroarenes

Zahra Moradi[1] & Arash Ghorbani-Choghamarani[2]✉

In this paper, a new type of magnetic mesoporous material (Fe_3O_4@SiO_2@KIT-6@2-ATP@Cu^I) was designed and synthesized and its application in the synthesis of amides and anilines was investigated. The structure of Fe_3O_4@SiO_2@KIT-6@2-ATP@Cu^I was characterized and identified using FTIR, SEM, XRD, TGA, BET, VSM, and ICP techniques. An external magnet can easily remove the synthesized catalyst from the reaction medium, and be reused in several consequence runs.

Functional anilines are versatile intermediates for the preparation of agricultural chemicals, pigments, pharmaceuticals, and dyes[1–8]. Because of their importance, many methods have been developed for the reduction of nitroarenes to produce corresponding anilines. Generally, the methods can be classified into two types. In the common procedure, the stoichiometric reduction of the corresponding nitroarenes occurred using an appropriate reducing agent such as $Na_2S_2O_4$, Fe, Sn, or Zn; this method often reasons environmental problems such as large amounts of waste acids and residues produced during the reaction. In the second procedure, the hydrogenation of nitro compounds is performed by metal catalysts in the presence of an appropriate catalyst[9–11].

Amides are important raw materials for the production of detergents, lubricants, drug stabilizers, and mediators in peptide and protein synthesis[12–18]. For preparing amides from nitriles different methods have been reported in the literature, hydration of nitriles to the corresponding amides is one of the extensively studied procedures[19–24].

Today, the use of magnetic nanoparticles (MNPs) in catalytic reactions is wildly studied. Magnetic mesoporous silica (MMS) nanoparticles due to their many important properties such as excellent stability (thermal and chemical), high surface area, simple and easy separation from the reaction medium, and recyclability, show excellent catalytic performance in a wide range of organic reactions[25–28]. In this research project, we have synthesized a new and efficient catalyst (Fe_3O_4@SiO_2@KIT-6@2-ATP@Cu^I) that has the advantage of both magnetic nanoparticles and mesoporous materials. In this research, the catalytic aspects of Fe_3O_4@SiO_2@KIT-6@2-ATP@Cu^I have been examined for hydrating nitriles and reducing nitroarenes.

Result and discussion

Preparation and characterization of Fe_3O_4@SiO_2@KIT-6@2-ATP@Cu^I. The Fe_3O_4@SiO_2@KIT-6 was prepared as mentioned procedure in our newly published work[29]. Subsequently, the prepared nanoparticles were first functionalized by (3-chloropropyl) trimethoxysilane and then reacted with 2-amino thiophenol. Finally, Cu(I) was coordinated with Fe_3O_4@SiO_2@KIT-6@2-ATP (Fig. 1).

After designing and fabricating Fe_3O_4@SiO_2@KIT-6@2-ATP@Cu^I, the synthesized magnetic mesoporous structure was characterized by different techniques.

Infrared spectroscopy is one of the most widely used analyses for the identification of different functional groups of organic compounds. Various devices have been developed for infrared spectroscopy, the most widely used of which are Fourier transform devices. Therefore, Fourier transforms infrared spectroscopy (FT-IR) was used to identify the synthesized catalyst[30]. In Fig. 2, the synthetic steps of magnetic mesoporous catalyst have been studied by FT-IR analysis. Peaks appearing in 459 cm^{-1}, 457 cm^{-1}, 462 cm^{-1}, 460 cm^{-1}, 640 cm^{-1}, 635 cm^{-1}, and 634 cm^{-1} in the spectra of Fe_3O_4@SiO_2@KIT-6 (Fig. 2a), Fe_3O_4@SiO_2@KIT-6@CPTMS (Fig. 2b), Fe_3O_4@SiO_2@KIT-6@2-ATP (Fig. 2c) and Fe_3O_4@SiO_2@KIT-6@2-ATP@Cu^I (Fig. 2d) is related to the stretching vibration of the Fe–O bond. Also, the stretching vibration of the Si–O–Si bond in the region of 1077–1083 cm^{-1} appears in

[1]Department of Chemistry, Faculty of Sciences, Ilam University, P.O. Box 69315516, Ilam, Iran. [2]Department of Organic Chemistry, Faculty of Chemistry, Bu-Ali Sina University, P.O. Box 6517838683, Hamedan, Iran. ✉email: a.ghorbani@basu.ac.ir; arashghch58@yahoo.com

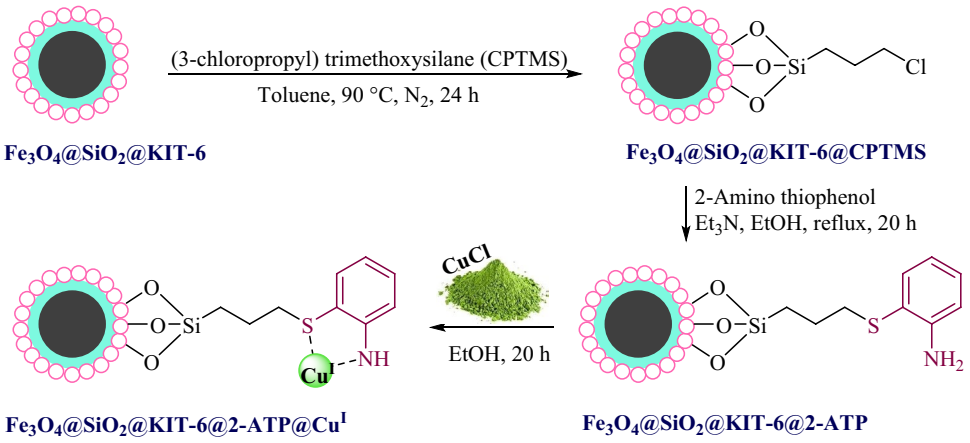

Figure 1. Stepwise preparation of Fe_3O_4@SiO_2@KIT-6@2-ATP@Cu^I.

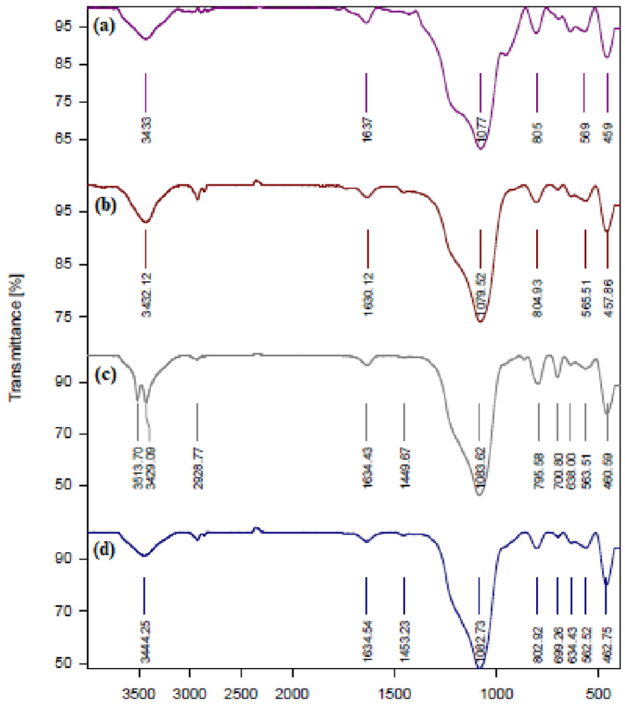

Figure 2. Infrared spectra of Fe_3O_4@SiO_2@KIT-6 (**a**), Fe_3O_4@SiO_2@KIT-6@CPTMS (**b**), Fe_3O_4@SiO_2@KIT-6@2-ATP (**c**), Fe_3O_4@SiO_2@KIT-6@2-ATP@Cu^I (**d**).

Fig. 2a–d. In the Fe_3O_4@SiO_2@KIT-6@2-ATP spectrum (Fig. 2c), the peak is shown in 3513 cm^{-1} and 3429 cm^{-1} corresponding to the NH stretching vibration. In the spectrum, Fe_3O_4@SiO_2@KIT-6@2-ATP@Cu^I (Fig. 2d) the peak that appears at 3444 cm^{-1} is belong to the N–H stretching vibration.

Scanning electron microscope (SEM) is one of the most common tools used in nanotechnology to analyze the morphology of nanostructural materials. The bombardment of the sample causes electrons to be released from the sample towards the positively charged plate, where these electrons become signals. The movement of the beam on the sample provides a set of signals based on which the microscope can display an image of the sample surface on the computer screen. So, in general, it is possible to obtain information including topography, components, and morphology of the sample[31].

To consider the morphology and particle shape of the magnetic mesoporous catalyst, the SEM image of Fe_3O_4@SiO_2@KIT-6 (a), Fe_3O_4@SiO_2@KIT-6@CPTMS (b), Fe_3O_4@SiO_2@KIT-6@2-ATP (c), Fe_3O_4@SiO_2@KIT-6@2-ATP@Cu^I (d) has been prepared, which has been brought in Fig. 3. The SEM images confirm the mesoporous catalyst formed in spherical shapes.

Thermogravimetric analysis (TGA), using a specific heating program and under a controlled atmosphere, measures weight changes in air or an inert atmosphere and records the mass reduction as a function of increasing

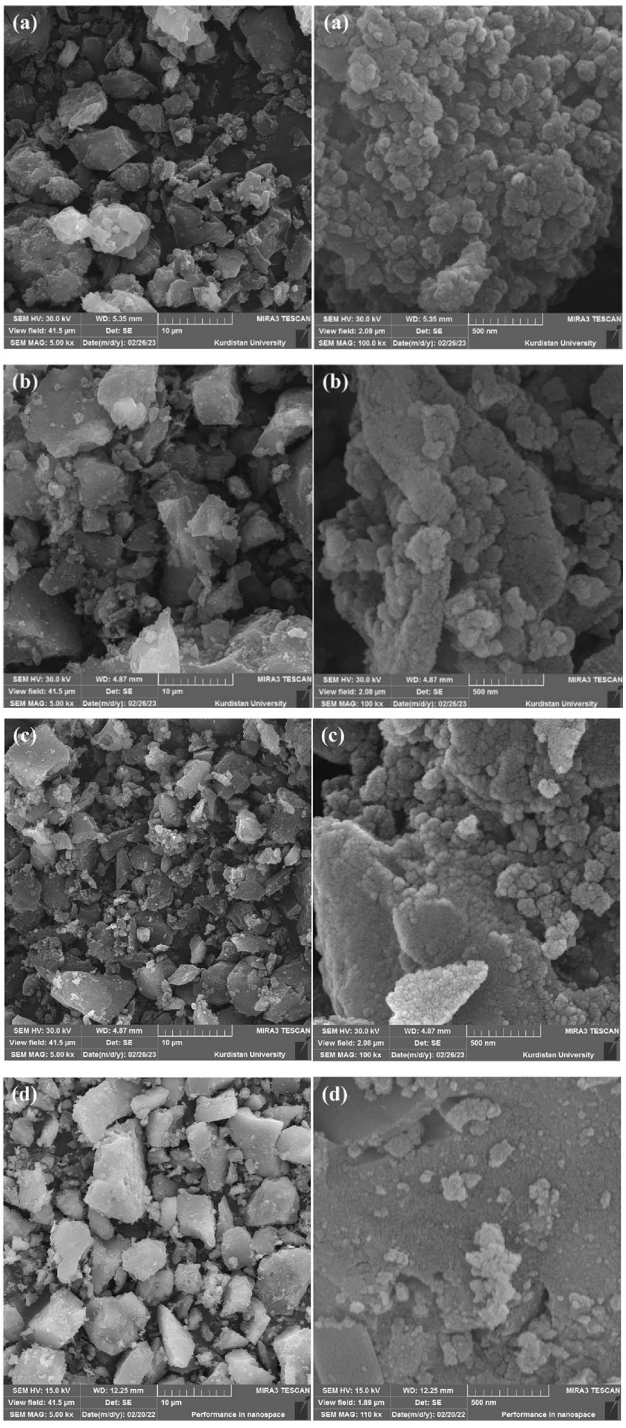

Figure 3. SEM image of Fe_3O_4@SiO_2@KIT-6 (**a**), Fe_3O_4@SiO_2@KIT-6@CPTMS (**b**), Fe_3O_4@SiO_2@KIT-6@2-ATP (**c**), Fe_3O_4@SiO_2@KIT-6@2-ATP@Cu^I (**d**).

temperature. Based on the results of thermal gravimetric analysis, it is possible to calculate the amount of combustible or vaporizable materials, including water and organic materials of the sample[32].

Figure 4 shows the TGA diagram of a catalyst activated with 2-amino thiophenol. According to the diagram, the first weight loss (under 250 °C, about 3%) is related to the evaporation of adsorbed solvents. The second weight loss, which is about 12% and occurred at temperatures between 250 to 650 °C, is related to the removal of immobilized organic compounds, indicating that 2-amino thiophenol was successfully immobilized into KIT-6 magnetic channels.

The X-ray diffraction pattern for the Fe_3O_4@SiO_2@KIT-6@2-ATP@Cu^I catalyst is shown in Figs. 5 and 6, (low and wide angle respectively). The low-angle XRD spectrum shows in Fig. 5. In the high-angle XRD spectrum

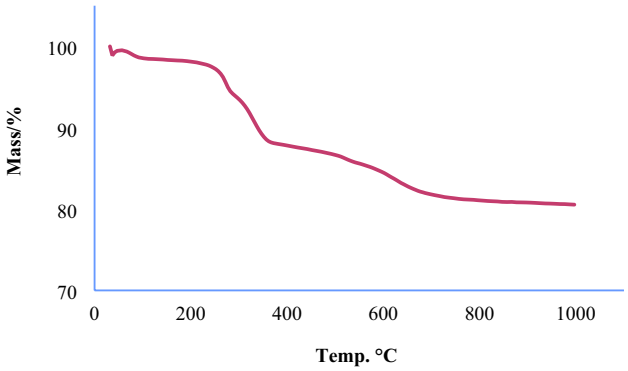

Figure 4. TGA diagram of Fe_3O_4@SiO_2@KIT-6@2-ATP@Cu^I.

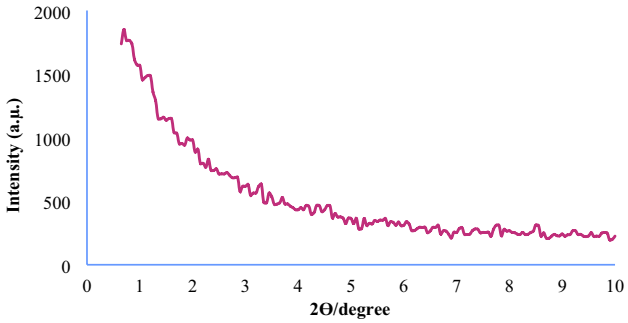

Figure 5. XRD patterns of Fe_3O_4@SiO_2@KIT-6@2-ATP@Cu^I (low angle XRD).

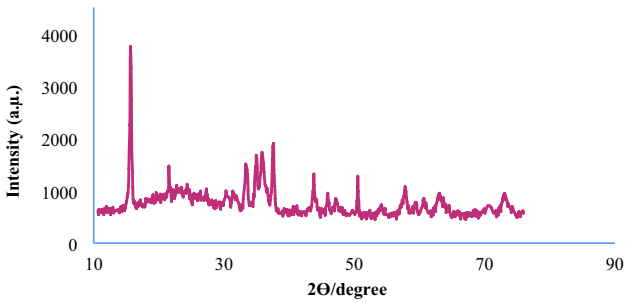

Figure 6. XRD patterns of Fe_3O_4@SiO_2@KIT-6@2-ATP@Cu^I (wide angle XRD).

(Fig. 6), the peaks appearing at 43.79°, 50.54°, and 73.24° correspond to the copper metal-stabilized into the channels of the catalyst, and a broad peak of 20–30 is related to the amorph silica layer[33,34].

Figure 7 shows the nitrogen adsorption/desorption isotherm of Fe_3O_4@SiO_2@KIT-6@2-ATP@Cu^I. The isothermal adsorption–desorption curve for Fe_3O_4@SiO_2@KIT-6@2-ATP@Cu^I shows type IV of IUPAC isotherms, indicating the magnetic material form in a mesoporous structure. The N_2 adsorption–desorption isotherm had a sharp bend at P/P_0, indicating capillary density in uniform mesopores.

The pore and surface properties of Fe_3O_4@SiO_2@KIT-6@2-ATP@Cu^I were calculated and considered using a Brunauer-Emmet-Teller (BET) and Barret-Joyner-Halenda (BJH) methods (Tables 1 and 2).

As shown in Fig. 8, the magnetic property of Fe_3O_4@SiO_2@KIT-6@2-ATP@Cu^I (1.38 emu/g) shows a significant decrease compared to Fe_3O_4@SiO_2@KIT-6 nanoparticles (3.30 emu/g). The magnetic property of the mesoporous catalyst reflects the fact that the surface of the nanoparticles is coated with SiO_2 and organic groups.

ICP analysis was used to determine the exact amount of loaded Cu on the magnetic mesoporous catalyst and showed a value of 1.11×10^{-3} mol/g.

Catalytic studies. *Hydration of benzonitriles to amides.* After the structure characterized the magnetic mesoporous catalyst, its catalytic activity in the synthesis of amides was investigated. The reaction of 4-chlorobenzonitrile as model substrate was investigated in the presence of potassium hydroxide, various solvents

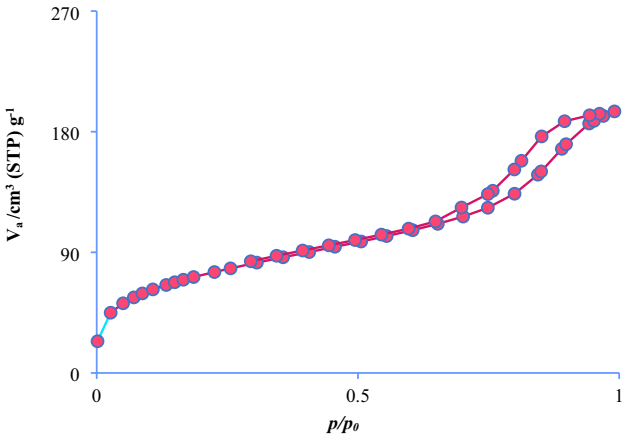

Figure 7. N_2 adsorption–desorption isotherm of Fe_3O_4@SiO_2@KIT-6@2-ATP@Cu^I.

Vm	58.016 cm^3g^{-1}
$a_{s, BET}$	252.51 m^2g^{-1}
Total pore volume(p/p = 0.990)	0.3016 cm^3g^{-1}
Mean pore diameter	4.78 nm

Table 1. Nitrogen adsorption–desorption data was calculated by the BET method, for mesoporous magnetic catalyst (Fe_3O_4@SiO_2@KIT-6@2-ATP@Cu^I).

V_p	**0.2491 cm^3g^{-1}**
r_p, peak(area)	1.22 nm
a_p	157.52 m^2g^{-1}

Table 2. BJH-plot data for Fe_3O_4@SiO_2@KIT-6@2-ATP@Cu^I.

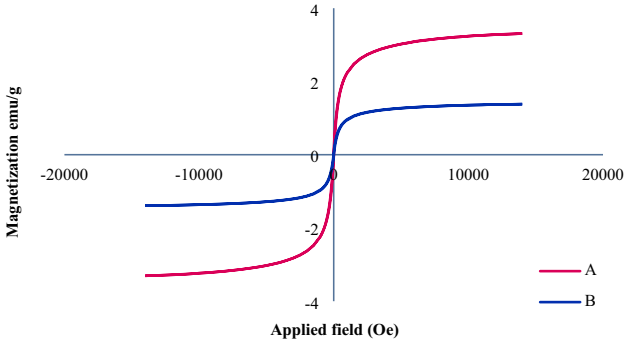

Figure 8. The magnetic curve of Fe_3O_4@SiO_2@KIT-6 (**A**) and Fe_3O_4@SiO_2@KIT-6@2-ATP@Cu^I (**B**).

such as water, ethanol, methanol, tetrahydrofuran, and 1-propanol, variable amounts of catalyst, and different temperature conditions. In protic polar solvents, coordination between the solvent and benzonitrile with the catalyst activates the cyano group in the nitrile substrate. Among protic polar solvents, 1-propanol led to more amide formation due to its coordination with the substrate[33,35]. Finally, 1-propanol, 40 mg of catalyst, 70 °C temperature, and 2 mmol of potassium hydroxide were selected as optimal conditions (Table 3).

After obtaining the reaction conditions, the reaction of different benzonitriles was performed under optimal conditions and a variety of amides were synthesized (Fig. 9). The results including reaction times and yields are reported in Table 4.

The hydration mechanism in the presence of Fe_3O_4@SiO_2@KIT-6@2-ATP@Cu^I is proposed in Fig. 10. Initially, the coordination of benzonitrile with the copper atom from the catalyst may lead to an increase in the

Entry	Solvent	Catalyst (mg)	KOH (mmol)	Temperature (°C)	Time (min)	Yield (%) [a]
1	EtOH	40	2	70	120	46
2	MeOH	40	2	Reflux	120	61
3	H_2O	40	2	70	120	59
4	1-Propanol	40	2	70	120	94
5	THF	40	2	Reflux	120	70
6	1-Propanol	40	3	70	120	89
7	1-Propanol	40	4	70	120	87
8	1-Propanol	30	2	70	120	84
9	1-Propanol	20	2	70	120	79
10	1-Propanol	40	2	80	120	94
11	1-Propanol	40	2	60	120	83

Table 3. Optimization of conditions for the synthesis of amides in the presence of Fe_3O_4@SiO_2@KIT-6@2-ATP@Cu^I catalyst. [a]Isolated yield.

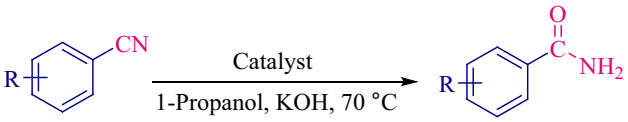

R: H, 4-NO_2, 3-NO_2, 4-Cl, 4-Br, 4-CN, 3-CN

Figure 9. Hydration of benzonitriles to amides.

electrophilicity of the nitrile carbon (intermediate I), which by the addition of HO^- ion leads to producing intermediate (III). Finally, the tautomerism of coordinated imines leads to an amide (IV)[36].

Reduction of nitroarenes to anilines. In another catalytic study, the activity of Fe_3O_4@SiO_2@KIT-6@2-ATP@Cu^I in the reduction of nitroarenes to aromatic amines was investigated (Table 5). After considering the effect of different solvents, temperature conditions, and different amounts of catalyst; water as the solvent, and room temperature were selected as the optimal conditions for the preparation of anilines from nitroarenes.

The effect of solvent on the reduction of nitroarenes was analyzed through articles and the results show that protic polar solvents are more suitable solvents for the reduction of nitroarenes than aprotic polar solvents[5].

After obtaining the optimal conditions, the reduction of different derivatives of nitroarenes to aromatic amines was performed and the results can be seen in Table 6 (Fig. 11).

A proposed mechanism for the reduction of nitro compounds in the presence of Fe_3O_4@SiO_2@KIT-6@2-ATP@Cu^I is provided in Fig. 12 [37].

Reusability of the catalyst. To investigate the recovery of described catalyst, the reduction reaction of 1-chloro-4-nitrobenzene was selected as the sample reaction. The reaction was selected using 1-chloro-4-nitrobenzene, sodium borohydride, and water as the solvent in the presence of Fe_3O_4@SiO_2@KIT-6@2-ATP@Cu^I. After the reaction was complete, it was separated by an external magnetic field, washed with ethanol and water, and then used in the next run. This cycle was repeated up to four times (Fig. 13).

Conclusions

In this paper, the Fe_3O_4@SiO_2@KIT-6@2-ATP@Cu^I as a magnetic mesoporous catalyst was designed and synthesized through the combination of Fe_3O_4 and KIT-6 nanoparticles. The catalytic ability of this mesoporous magnetic material was studied for the preparation of benzamides and anilines. The reported procedure in this research project offers the advantages of reasonable yields and green reaction medium, versatile catalyst preparation procedure, short reaction times of catalytic reactions, easy separation (it could be easily separated and recovered due to its magnetic properties), catalyst recyclability, and high catalyst chemical stability.

In Table 7, the Fe_3O_4@SiO_2@KIT-6@2-ATP@Cu^I magnetic catalyst was compared with other previously reported catalysts for the reduction of nitrobenzene. As is evidenced in this table, the obtained results by the described catalyst in this research are comparable with other reductive systems.

Experimental

Synthesis of Fe_3O_4@SiO_2@KIT-6@2-ATP. Fe_3O_4@SiO_2@KIT-6 nanoparticles were synthesized using a method previously reported in the literature[38]. In a 50 mL balloon, Fe_3O_4@SiO_2@KIT-6 (1 g) was sonicated for 30 min in toluene (25 mL), then, 1.5 mL of (3-chloropropyl) trimethoxysilane (CPTMS) was added and the resulting mixture was stirred for 24 h at 90 °C under nitrogen atmosphere. The obtained solid was washed with

Entry	Benzonitrile	Product	Time (min)	Yield (%)	Melting point (°C)
1	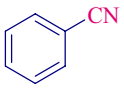	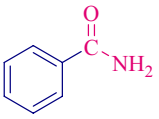	120	94	121–124[16]
2	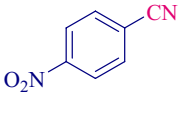	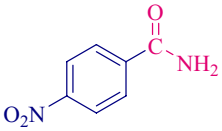	120	90	199–200[36]
3	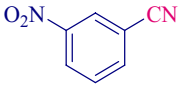	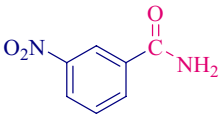	120	91	142–143[36]
4	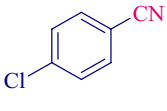	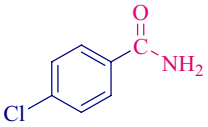	120	94	171–173[15]
5		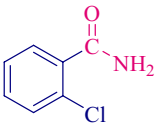	120	90	135–137[15]
6	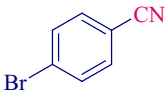	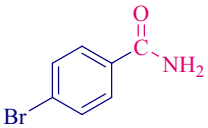	120	91	190–192[16]
7	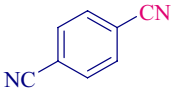	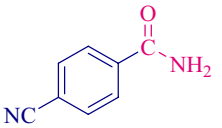	50	87	180–182[36]
8	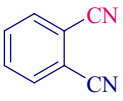	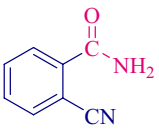	52	88	224–225[36]

Table 4. Synthesis of amides from benzonitriles in the presence of Fe_3O_4@SiO_2@KIT-6@2-ATP@Cu^I catalyst. Reaction conditions: 4-Chlorobenzonitrile (1 mmol), potassium hydroxide (2 mmol), 1-Propanol, temperature, catalyst 40 mg.

dichloromethane (50 mL) and dried in an oven. In a round bottom balloon, a mixture of Fe_3O_4@SiO_2@KIT-6@CPTMS (1 g), and one gram of 2-amino thiophenol (2-ATP) was refluxed in the presence of triethylamine (2 mL) in ethanol for 20 h. After separating the obtained precipitate and washing it with ethanol, it was dried at 50 °C[39].

Synthesis of Fe_3O_4@SiO_2@KIT-6@2-ATP@Cu^I. The solid precipitate that was obtained in the previous step, was dissolved in ethanol and 2 mmol of CuCl was added and refluxed for 20 h. After the end of the reaction, the Fe_3O_4@SiO_2@KIT-6@2-ATP@Cu^I catalyst was separated and washed several times with ethanol[40].

The general method for the hydration of benzonitriles to amides. To perform hydration of benzonitrile, in a 5 mL round bottom flask, benzonitrile (1 mmol), potassium hydroxide (2 mmol), and 40 mg of Fe_3O_4@SiO_2@KIT-6@2-ATP@Cu^I were added to 1-propanol and the mixture was stirred at 70 °C. The progress of the reaction was followed by TLC. After the completion reaction, the catalyst was separated by an external magnet and the corresponding product was extracted.

4-Cyanobenzamide. ^{1}HNMR (300 MHz, DMSO-*d6*) δ 8.01 (2H, d, J = 8 Hz), 7.95 (2H, d, J = 8 Hz), 7.66 (s, 2H).

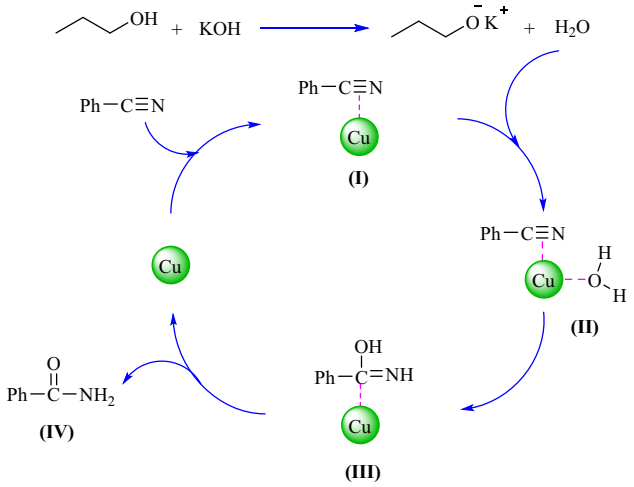

Figure 10. The suggested mechanism of amide synthesis in the presence of Fe_3O_4@SiO_2@KIT-6@2-ATP@Cu^I as a catalyst.

Entry	Solvent	Catalyst (mg)	$NaBH_4$ (mmol)	Time (min)	Yield (%)[a]
1	H_2O	10	5	40	82
2	H_2O	15	5	40	84
3	H_2O	20	5	40	92
4	EtOH	20	5	40	81
5	H_2O:EtOH	20	5	40	79
6	H_2O	20	4	40	83
7	H_2O	20	3	40	75
8	CH_3CN	20	5	40	31
9	MeOH	20	5	40	49

Table 5. Optimization of reaction conditions in the presence of Fe_3O_4@SiO_2@KIT-6@2-ATP@Cu^I catalyst. [a]Isolated yield.

4-Nitrobenzamide. ^{1}HNMR (300 MHz, DMSO-*d*6) δ 8.28 (2H, d, J = 8.1), 8.08 (2H, d, J = 8.1), 7.71 (s, 2H).

The general method for the reduction of nitroarenes to anilines. To prepare anilines from nitroarenes, a mixture of nitroarene, $NaBH_4$ (5 mmol), and 20 mg catalyst was stirred at room temperature. TLC was used to monitor the progress of the reaction and the product was obtained in high yield after catalyst isolation.

4-Bromoaniline. ^{1}HNMR (300 MHz, $CDCl_3$): δ 7.23 (2H, d, J = 7 Hz), 6.57 (2H, d, J = 7 Hz), 3.53 (s, 2H).

2-Aminobenzyl alcohol. ^{1}HNMR (300 MHz, $CDCl_3$): δ 6.93–7.05 (m, 2H), 6.49–6.62 (m, 2H), 4.95 (s, 1H), 4.87 (s, 2H), 4.38 (s, 2 H) (Supplementary Information).

Entry	Nitro arene	Product	Time (min)	Yield (%)[a]	Melting point (°C)
1	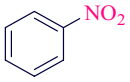	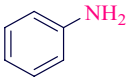	60	89	Oil[3]
2	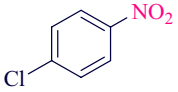	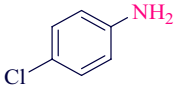	40	92	68–70[33]
3	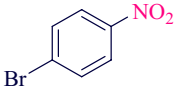	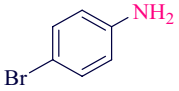	35	90	64–65[41]
4	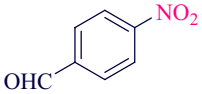	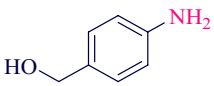	32	90	85–88[41]
5	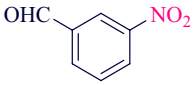	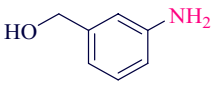	32	90	85–86[41]
6	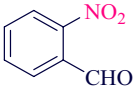	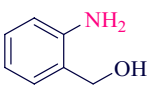	35	90	79–81[41]
7	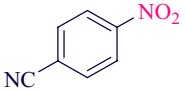	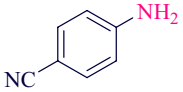	20	92	79–80[42]
8	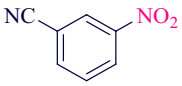	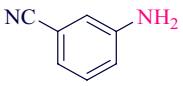	28	91	52–53[42]

Table 6. Synthesis of anilines from the reduction of nitroarenes Fe_3O_4@SiO_2@KIT-6@2-ATP@Cu^I catalyst. Reaction conditions: 4-Chlorobenzene (1 mmol), $NaBH_4$ (5 mmol), room temperature, catalyst 20 mg. [a]Isolated yield.

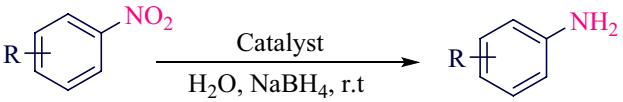

R: H, 4-Cl, 4-Br, 4-CHO, 3-CHO, 2-CHO, 4-CN, 3-CN

Figure 11. Reduction of nitroarenes to anilines.

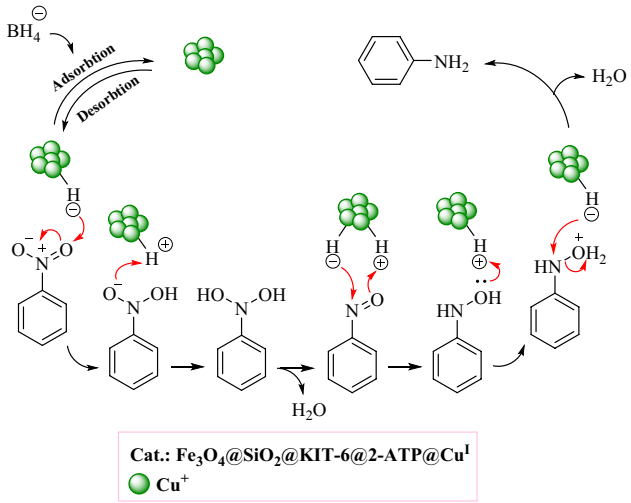

Figure 12. A suggested mechanism for the reduction of nitro compounds by $NaBH_4$ in the presence of a catalytic amount of Fe_3O_4@SiO_2@KIT-6@2-ATP@Cu^I.

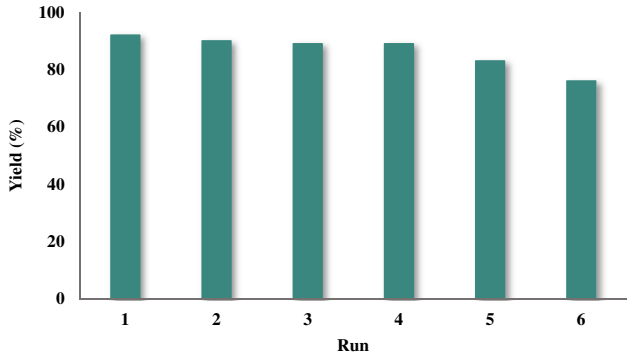

Figure 13. Catalyst recovery study.

Entry	Catalyst	Conditions	Time (h)	Yield (%)[a]	Ref
1	SB-Pd@MNPs	H_2O, r.t, $NaBH_4$	0.03	92	[43]
2	Pd/PPh_3@FDU-12	EtOH, 40 °C, 10 bar H_2	1	99	[29]
3	SiO_2@APTES@β-CD@Pd-PDR	H_2O, r.t, $NaBH_4$	3	99	[44]
4	Co–N/C-800	EtOH, 100 °C, H_2	4	96	[45]
5	$[Co(\kappa S,N\text{-tfmp2S})_3]$	MeOH, 40 °C, $MeNHNH_2$	4	92	[46]
6	Fe_3O_4@SiO_2@KIT-6@ 2-ATP@Cu^I	H_2O, r.t, $NaBH_4$	1	89	This work

Table 7. Comparison of Fe_3O_4@SiO_2@Kit-6@2-ATP@Cu^I with other catalysts for the reduction of nitrobenzene. [a]Isolated yield.

Data availability

All data generated or analyzed during this study are included in this published article [and its supplementary information files].

Received: 8 January 2023; Accepted: 29 April 2023
Published online: 11 May 2023

References

1. Shi, Y. *et al.* Pt decorated hierarchical Sb_2WO_6 microspheres as a surface functionalized photocatalyst for the visible-light-driven reduction of nitrobenzene to aniline. *J. Mater. Chem. A* **8**, 18755–18766 (2020).

2. Babel, V. & Hiran, B. L. Heterogeneous AgPd alloy nanocPt decorated hierarchical Sb_2WO_6 microspheres as a surface functionalized photocatalyst for the visible-light-driven reduction of nitrobenzene to anilineatalyst for selective reduction of aromatic nitro compounds using formic. *Catal. Lett.* **150**, 1865–1869 (2020).
3. Singh, P., Halder, M., Ray, S., Bandyopadhyay, B. & Sen, K. Biomolecule-mediated generation of Ru nanocatalyst for sustainable reduction of nitrobenzene. *ACS Omega* **4**, 21267–21278 (2019).
4. Romanazzi, G. *et al.* Polymer supported nickel nanoparticles as recyclable catalyst for the reduction of nitroarenes to anilines in aqueous medium. *Mol. Catal.* **446**, 31–38 (2018).
5. Niakan, M. & Asadi, Z. Selective reduction of nitroarenes catalyzed by sustainable and reusable DNA-supported nickel nanoparticles in water at room temperature. *Catal. Lett.* https://doi.org/10.1007/s10562-019-02741-7 (2019).
6. Zhang, Q. *et al.* Highly efficient hydrogenation of nitrobenzene to aniline over Pt/CeO_2 catalysts: The shape effect of the support and key role of additional Ce^{3+} sites. *ACS Catal.* **10**, 10350–10363 (2020).
7. Krogul-Sobczak, A., Cedrowski, J., Kasperska, P. & Litwinienko, G. Reduction of nitrobenzene to aniline by Co/H_2O in the presence of palladium nanoparticles. *Catalysts* **9**, 404 (2019).
8. Wang, H., Liu, X., Xu, G., Guo, Z. & Zhang, Y. In situ synthesis of Fe–N–C catalysts from cellulose for hydrogenation of nitrobenzene to aniline. *Chinese J. Catal.* **40**, 1557–1565 (2019).
9. Bao, L. *et al.* Palladium supported on metal–organic framework as a catalyst for the hydrogenation of nitroarenes under mild conditions. *Appl. Organomet. Chem.* **34**, 1–8 (2020).
10. Zubar, V., Dewanji, A. & Rueping, M. Chemoselective hydrogenation of nitroarenes using an air-stable base-metal catalyst. *Org. Lett.* **23**, 2742–2747 (2021).
11. Manrique, E. *et al.* A heterogeneous ruthenium dmso complex supported onto silica particles as a recyclable catalyst for the efficient hydration of nitriles in aqueous medium. *Inorg. Chem.* **58**, 8460–8470 (2019).
12. Kumar Reddy, N. N., Nageswara Rao, S. D., Patil, R. & Adimurthy, S. Transition metal-free hydration of nitriles to amides mediated by NaOH. *Adv. Mater. Sci.* **3**, 1–7 (2018).
13. Xing, X. *et al.* Highly active platinum catalysts for nitrile and cyanohydrin hydration: Catalyst design and ligand screening via high-throughput techniques. *J. Am. Chem. Soc.* **140**, 17782–17789 (2018).
14. Xu, D. P., Xiong, M. & Kazemnejadi, M. Efficient reduction of nitro compounds and domino preparation of 1-substituted-1H-1,2,3,4-tetrazoles by Pd(II)-poly salophen coated magnetite NPs as a robust versatile nanocomposite. *RSC Adv.* **11**, 12484–12499 (2021).
15. Sanz Sharley, D. D. & Williams, J. M. J. A selective hydration of nitriles catalysed by a Pd(OAc)2-based system in water. *Tetrahedron Lett.* **58**, 4090–4093 (2017).
16. Sultana, S., Borah, G. & Gogoi, P. K. Ru (III) Schiff-base complex anchored on nanosilica as an efficient and retrievable catalyst for hydration of nitriles. *Appl. Organomet. Chem.* **33**, 1–11 (2019).
17. Guo, B. & De Vries, J. G. Hydration of nitriles using a metal-ligand cooperative ruthenium pincer catalyst. *Chem. Sci.* **10**, 10647–10652 (2019).
18. Kuwabara, J., Sawada, Y. & Yoshimatsu, M. Nitrile hydration reaction using copper iodide/cesium carbonate/DBU in nitromethane-water. *Synletter* **29**, 2061–2065 (2018).
19. Wang, H. *et al.* Nanorod manganese oxide as an efficient heterogeneous catalyst for hydration of nitriles into amides. *Ind. Eng. Chem. Res.* **58**, 17319–17324 (2019).
20. Wang, N., Ma, P., Xie, J. & Zhang, J. Transition metal-free NaOH-catalyzed hydration of nitriles to primary amides in $NH_3{\cdot}H_2O$–DMSO mixture. *Mol. Divers.* **25**, 1131–1136 (2021).
21. Hussain, M. A. *et al.* An efficient hydration of nitriles with ruthenium-supported heterogeneous catalyst in water under moderate conditions. *J. Ind. Eng. Chem.* **99**, 187–195 (2021).
22. Czégéni, C.E., De, S., Udvardy, A., Derzsi, N.J., Papp, G. & Joó, F. Selective Hydration of Nitriles to Corresponding Amides in Air with Rh (I)-N-Heterocyclic Complex Catalysts. *Catalysts.* **10**(1), 125 (2020).
23. Rahman, T., Borah, G. & Gogoi, P. K. Activated Mont K10-Carbon supported Fe_2O_3: A versatile catalyst for hydration of nitriles to amides and reduction of nitro compounds to amines in aqueous media. *J. Chem. Sci.* **133**, 20–22 (2021).
24. KazemiMiraki, M., Arefi, M., Salamatmanesh, A., Yazdani, E. & Heydari, A. Magnetic nanoparticle-supported Cu–NHC complex as an efficient and recoverable catalyst for nitrile hydration. *Catal. Lett.* **148**, 3378–3388 (2018).
25. Asgari, M., Soleymani, M., Miri, T. & Barati, A. A robust method for fabrication of monodisperse magnetic mesoporous silica nanoparticles with core-shell structure as anticancer drug carriers. *J. Mol. Liq.* **292**, 111367 (2019).
26. Adam, A. *et al.* Orienting the pore morphology of core-shell magnetic mesoporous silica with the sol–gel temperature. Influence on MRI and magnetic hyperthermia properties. *Molecules* **26**, 971 (2021).
27. He, H. *et al.* Thiol-ene click chemistry synthesis of a novel magnetic mesoporous silica/chitosan composite for selective Hg(II) capture and high catalytic activity of spent Hg(II) adsorbent. *Chem. Eng. J.* **405**, 126743 (2021).
28. Abdolmohammadi, S., Shariati, S. & Mirza, B. Ultrasound promoted and Kit-6 mesoporous silica-supported Fe3O4 magnetic nanoparticles catalyzed cyclocondensation reaction of 4-hydroxycoumarin, 3,4-methylenedioxyphenol, and aromatic aldehydes. *Appl. Organomet. Chem.* **35**, 1–10 (2021).
29. Guo, M. *et al.* Improving catalytic hydrogenation performance of Pd nanoparticles by electronic modulation using phosphine ligands. *ACS Catal.* **8**, 6476–6485 (2018).
30. Undavalli, V. K., Ling, C., & Khandelwal, B. Impact of alternative fuels and properties on elastomer compatibility. in *Aviation Fuels*. 113–132 (Academic Press, 2021).
31. Nasrollahzadeh, M., Atarod, M., Sajjadi, M., Sajadi, S. M. & Issaabadi, Z. Plant-mediated green synthesis of nanostructures: Mechanisms, characterization, and applications. *Interface Sci. Technol.* **28**, 199–322 (2019).
32. Ebnesajjad, S. Surface and material characterization techniques. in *Handbook of Adhesives and Surface Preparation*. 31–48 (Elsevier, 2011).
33. Sultana, S., Geetika, B. & Pradip, K. G. Ru (III) Schiff-base complex anchored on nanosilica as an efficient and retrievable catalyst for hydration of nitriles. *Appl. Organomet. Chem.* **33**(1), e4595 (2019).
34. Amin, R., Khorshidi, A., Shojaei, A. F., Rezaei, S. & Faramarzi, M. A. Immobilization of laccase on modified Fe_3O_4@SiO_2@Kit-6 magnetite nanoparticles for enhanced delignification of olive pomace bio-waste. *Int. J. Biol. Macromol.* **114**, 106–113 (2018).
35. Yin, A. G. *et al.* Efficient bimetallic catalysis of nitrile hydration to amides by simple $Pd(OAc)_2$/Lewis acid catalyst at ambient temperature. *J. Organ. Chem. Eur.* https://doi.org/10.1002/ejoc.201601495 (2016).
36. Ghorbani-Choghamarani, A. & Taherinia, Z. Fe_3O_4@GlcA@Cu-MOF: A magnetic metal-organic framework as a recoverable catalyst for the hydration of nitriles and reduction of isothiocyanates, isocyanates, and isocyanides. *ACS Comb. Sci.* **22**, 902–909 (2020).
37. El-Hout, S. I. *et al.* A green chemical route for synthesis of graphene supported palladium nanoparticles: A highly active and recyclable catalyst for reduction of nitrobenzene. in *Applied Catalysis A: General*. Vol. 503 (Elsevier B.V., 2015).
38. Moradi, Z. & Ghorbani-Choghamarani, A. Design and synthesis of Fe_3O_4@SiO_2@KIT-6@DTZ-Pd0 as a new and efficient mesoporous magnetic catalyst in carbon–carbon cross-coupling reactions. *Sci. Rep.* **11**, 1–12 (2021).
39. Mousavi, S. H., Manoochehri, M. & Afshar Taromi, F. Fabrication of a novel magnetic metal-organic framework functionalized with 2-amino thiophenol for preconcentration of trace silver amounts in water and wastewater. *RSC Adv.* **11**, 13867–13875 (2021).

40. Ghorbani-Choghamarani, A., Sahraei, R., Taherinia, Z. & Mohammadi, M. Cu(I)@Isatin-glycine-boehmite nanoparticles: As novel heterogeneous catalyst for the synthesis and selective oxidation of sulfides. *J. Iran. Chem. Soc.* **18**, 827–838 (2021).
41. Zeynizadeh, B. & Sepehraddin, F. Synthesis and characterization of magnetically nanoparticles of Fe_3O_4@APTMS@$ZrCp_2$ as a novel and reusable catalyst for convenient reduction of nitro compounds with glycerol. *J. Iran. Chem. Soc.* **14**, 2649–2657 (2017).
42. Chen, D. *et al.* Metal-free reduction of nitro aromatics to amines with $B_2(OH)_4/H_2O$. *Synletter* **29**, 1765–1768 (2018).
43. Manjunatha, K. *et al.* Magnetic nanoparticle-tethered Schiff base–palladium(II): Highly active and reusable heterogeneous catalyst for Suzuki-Miyaura cross-coupling and reduction of nitroarenes in aqueous medium at room temperature. *Appl. Organomet. Chem.* **32**, 1–21 (2018).
44. Feng, X. P. *et al.* Immobilized β-cyclodextrin and palladium-pyridylaldehyde complex on silica nanoparticles as a highly active catalyst for Suzuki, reduction of nitroarenes and oxidative amination of aldehydes reactions in water. *Mater. Today Commun.* **26**, 101909 (2021).
45. Dai, Y., Li, X., Wang, L. & Xu, X. Highly efficient hydrogenation reduction of aromatic nitro compounds using MOF derivative Co-N/C catalyst. *New J. Chem.* **45**, 22908–22914 (2021).
46. Ioannou, D. I. *et al.* Selective reduction of nitroarenes to arylamines by the cooperative action of methylhydrazine and a tris(*N*-heterocyclic thioamidate) cobalt(III) complex. *J. Org. Chem.* **86**, 2895–2906 (2021).

Acknowledgements

This work was supported by the research facilities of Ilam University and Bu-Ali Sina University.

Author contributions

Z.M.: Methodology, Validation, Methodology, Investigation, Writing-original draft. A.G.-C.: Funding acquisition, Supervision, Conceptualization, Resources, Writing-review & editing.

Competing interests

The authors declare no competing interests.

Additional information

Supplementary Information The online version contains supplementary material available at https://doi.org/10.1038/s41598-023-34409-z.

Correspondence and requests for materials should be addressed to A.G.-C.

Reprints and permissions information is available at www.nature.com/reprints.

Publisher's note Springer Nature remains neutral with regard to jurisdictional claims in published maps and institutional affiliations.